Propene Polymerization with the Isospecific, Highly Regiospecific *rac*-$Me_2C(3\text{-}t\text{-}Bu\text{-}1\text{-}Ind)_2ZrCl_2$/MAO Catalyst. 1. Influence of Hydrogen on Initiation and Propagation: Experimental Detection and Theoretical Investigation of 2,1 Propene Insertion into the Zr−H Bond[1]

Gilberto Moscardi, Fabrizio Piemontesi, and Luigi Resconi*

Montell Polyolefins, Centro Ricerche G. Natta, 44100 Ferrara, Italy

Received June 25, 1999

The influence of molecular hydrogen on propene polymerization promoted by the regio- and isospecific *rac*-$Me_2C(3\text{-}t\text{-}Bu\text{-}1\text{-}Ind)_2ZrCl_2$/MAO catalytic system has been investigated both by experiment (liquid propene, T_p = 50 °C) and molecular modeling (quantum mechanics/molecular mechanics). A competitive secondary (2,1) propene insertion into the Zr−H bond, originated after chain transfer to hydrogen, is detected by ^{13}C NMR analysis of these polymers: increasing amounts of the new $CH_3-CH(CH_3)-CH(CH_3)-CH_2-$ chain-end group are observed when the hydrogen partial pressure is increased from 1 to 4 bar. The ratio between primary (1,2) and secondary initiations is found to be constant and nearly equal to 5. On the other hand, the complete regiospecificity of propene insertion during chain propagation is preserved. A combined quantum mechanics/molecular mechanics study on the model cation [*rac*-$H_2C(3\text{-}t\text{-}Bu\text{-}1\text{-}Ind)_2Zr-H(propene)]^+$ shows that secondary propene coordination, followed by secondary insertion into the Zr−H bond which generates the observed structure of the saturated end group, is even favored over primary coordination/insertion, thanks to a stabilizing β-agostic bond between the metal center and one methyl hydrogen of the secondary coordinated propene. Two different mechanisms have been identified for primary propene insertion into the Zr(*n*-propyl) and Zr(isopropyl) species, with energy barriers of nearly 4 and 9 kcal/mol, respectively. The experimentally observed ratio of [1,2]/[2,1] $\approx$ 5 for initiations is explained in terms of side reactions that can transform the "slow" propagating Zr(isopropyl) site into the "fast" Zr(*n*-propyl) one. The model [*rac*-$H_2C(3\text{-}t\text{-}Bu\text{-}1\text{-}Ind)_2Zr(isopropyl)]^+$ cation shows indeed comparable energy barriers for monomer insertion and β-H transfer followed by associative displacement with a primary propene to generate the "fast" propagating species.

Introduction

Molecular hydrogen is the most used chain transfer agent for the control of polymer molecular weights in Ziegler−Natta polymerization of 1-olefins.[2,3] Chain transfer most likely occurs via direct addition of H_2 across the metal−polymer bond with formation of a saturated polymer chain and a metal−hydride bond:[4a−e]

$$L_nMR^+ + H_2 \longrightarrow \begin{matrix} H\cdots H \\ \vdots \quad \vdots \\ L_nM^{+}\cdots R \end{matrix} \longrightarrow L_nMH^+ + RH$$

Besides lowering the molecular weight of the polymer, addition of hydrogen generally causes an increase of polymerization activity using both heterogeneous[2] ($MgCl_2$/$TiCl_4$) and homogeneous[3] (metallocene) catalysts. The most common explanation of this activating effect is the

(1) Presented in part at the Workshop on "Advances in Olefin Polymerization with Organometallic Catalysts", Ferrara, May 28−29, 1998.

(2) (a) Guastalla, G.; Giannini, U. *Makromol. Chem., Rapid Commun.* **1983**, *4*, 519. (b) Hayashi, T.; Inoue, Y.; Chûjô, R.; Asakura, T. *Macromolecules* **1988**, *21*, 2675. (c) Parsons, I. W.; Al-Turki, T. M. *Polym. Commun.* **1989**, *30*, 72. (d) Kioka, M.; Kashiwa, N. *J. Macromol. Sci.-Part A (Chem.)* **1991**, *A28*, 865. (e) Guyot, A.; Spitz, R.; Dassaud, J. P.; Gomez, C. *J. Mol. Catal.* **1993**, *82*, 29. (f) Imaoka, K.; Ikai, S.; Tamura, M.; Yoshikiyo, M.; Yano, T. *J. Mol. Catal.* **1993**, *82*, 37. (g) Chadwick, J. C.; Miedema, A.; Sudmeijer, O. *Macromol. Chem. Phys.* **1994**, *195*, 167. (h) Albizzati, E.; Giannini, U.; Morini, G.; Galimberti, M.; Barino, L.; Scordamaglia, R. *Macromol. Symp.* **1995**, *89*, 73. (i) Bukatov, G. D.; Gancharov, V. S.; Zakharov, V. A. *Macromol. Chem. Phys.* **1995**, *196*, 1751. (j) Chadwick, J. C.; van Kessel, G. M. M.; Sudmeijer, O. *Macromol. Chem. Phys.* **1995**, *196*, 1431. (k) Kojoh, S.; Kioka, M.; Kashiwa, N.; Itoh, M.; Mizuno, A. *Polymer* **1995**, *36*, 5015. (l) Mori, H.; Tashino, K.; Terano, M. *Macromol. Chem. Phys.* **1995**, *196*, 651. (m) Chadwick, J. C.; Morini, G.; Albizzati, E.; Balbontin, G.; Mingozzi, I.; Cristofori, A.; Sudmeijer, O.; van Kessel, G. M. M. *Macromol. Chem. Phys.* **1996**, *197*, 2501. (n) Albizzati, E.; Giannini, U.; Balbontin, G.; Camurati, I.; Chadwick, J. C.; Dall'Occo, T.; Dubitsky, Y.; Galimberti, M.; Morini, G.; Maldotti, A. *J. Polym. Sci., Part A: Polym. Chem.* **1997**, *35*, 2645.

(3) (a) Tsutsui, T.; Kashiwa, N.; Mizuno, A. *Makromol. Chem., Rapid Commun.* **1990**, *11*, 565. (b) Busico, V.; Cipullo, R.; Chadwick, J. C.; Modder, J. F.; Sudmeijer, O. *Macromolecules* **1994**, *27*, 7538. (c) Jüngling, S.; Mülhaupt, R.; Stehling, U.; Brintzinger, H.-H.; Fischer, D.; Langhauser, F. *J. Polym. Sci. Part A: Polym. Chem.* **1995**, *33*, 1305. (d) Schupfner, G.; Kaminsky, W. *J. Mol. Catal. A* **1995**, *C102*, 59. (e) Carwill, A. Tritto, I. Locatelli, P., Sacchi, M. C. *Macromolecules* **1997**, *30*, 7056.

(4) (a) Brintzinger, H.-H. *J. Organomet. Chem.* **1979**, *171*, 337. (b) Gell, K. I.; Posin, B.; Schwartz, J.; Williams, G. *J. Am. Chem. Soc.* **1982**, *104*, 1846. (c) Wochner, F.; Brintzinger, H.-H. *J. Organomet. Chem.* **1986**, *309*, 65. (d) Guo, Z.; Bradley, P. K.; Jordan, R. F. *Organometallics* **1992**, *11*, 2690. (e) Ziegler, T.; Folga, E.; Berces, A. *J. Am. Chem. Soc.* **1993**, *115*, 636, and references therein.

10.1021/om990488g CCC: $18.00
Publication on Web 11/10/1999

Table 1. Propene Polymerization with 1/MAO in Liquid Propene at Different Hydrogen Levels[a]

sample	activity ($kg_{PP}/mmol_{Zr}$ h)	$p(H_2)$[b] (bar)	$\bar{M}_v$[c,d] (g/mol)	$\bar{M}_n$[e] (g/mol)	*mmmm*[f] (%)
1	44.3	0	88 000		94.9
2	47.5	1	50 100	32 000	95.1
3	81.3	2	42 100	19 000	95.0
4	61.7	3	15 200		
5	62.8	4		3200	93.2
6	41.0	4		2300	94.9

[a] Polymerization conditions: 1 L stainless steel autoclave, propene (0.4 L), 50 °C, 1 h, 0.5 mg of *rac*-[Me_2C(3-*t*-Bu-Ind)$_2$]$ZrCl_2$, solution zirconocene/MAO aged 10 min, Al/Zr = 5000 mol/mol. [b]Hydrogen partial pressure. [c]In THN, 135 °C. [d]From $[\eta] = K(M_v)^a$ with $K = 1.93 \times 10^{-4}$ and $\alpha = 0.74$. [e]From ^{13}C NMR (100 MHz). [f]Determined assuming the enantiomorphic site model.

regeneration of an active species from the "dormant sites" formed after a regioirregular olefin insertion.[2,3,5]

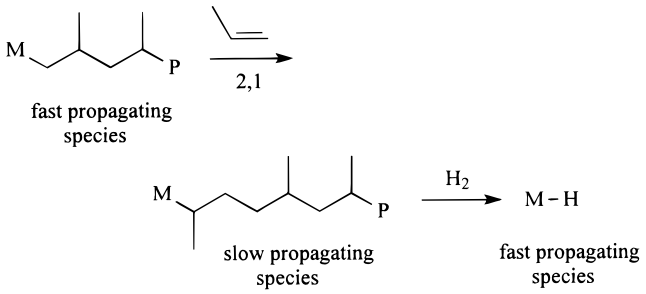

In fact, ^{13}C NMR spectra of polypropene samples prepared in the presence of hydrogen with Ziegler−Natta catalysts reveal the presence of a greater amount of *n-butyl groups*[2g,3a,5] (generated from chain transfer after a secondary insertion) with respect to *isobutyl groups* (from chain transfer after a primary insertion) as terminating polymer chain-end. The initiating polymer chain-end invariably present in these spectra is *n-propyl*, which is due to the 1,2 propene insertion in the metal−H bond.

We recently reported on the polymerization of propene with the *rac*-Me_2C(3-*tert*-butyl-1-indenyl)$_2ZrCl_2$/MAO (**1**/MAO) catalytic system,[6] which produces fully regioregular, highly isotactic polypropene (e.g., *mmmm* = 95%, T_m = 152 °C at T_p = 50 °C in liquid propene).

In this work we discuss the influence of hydrogen addition on liquid propene polymerization with **1**/MAO. The experimental results are compared with those from a combined quantum mechanics/molecular mechanics study on insertion and isomerization reactions.

Results and Discussion

Propene Polymerization and Analysis of Saturated End Groups. In Table 1 we report the polymerization conditions and the relevant results obtained in the polymerization of propene with *rac*-Me_2C(3-*t*-Bu-Ind)$_2ZrCl_2$/MAO in the presence of different amounts of hydrogen.

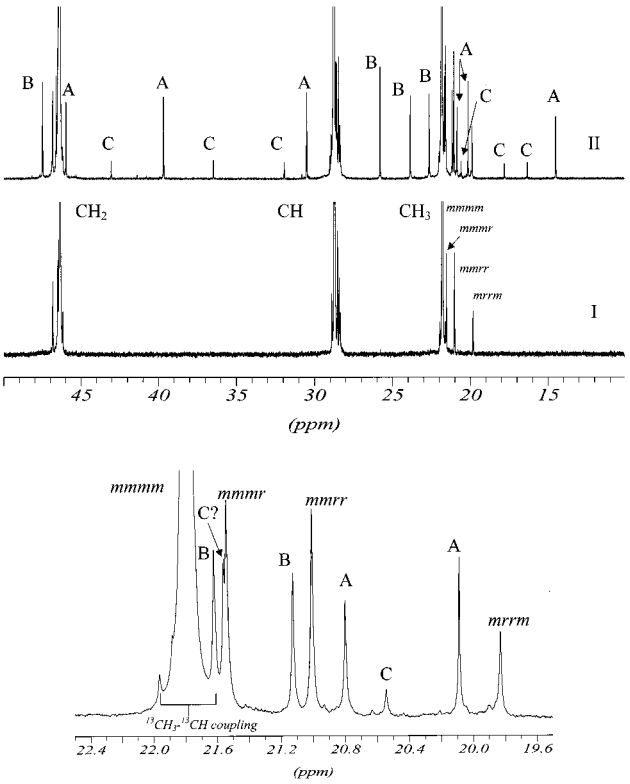

Figure 1. (a) ^{13}C NMR spectra of polypropenes prepared with Me_2C(3-*t*-Bu-Ind)$_2ZrCl_2$/MAO: I = sample 1, II = sample 6. End groups: A = *n*-propyl, B = isobutyl, C = 2,3-dimethylbutyl. (b) Expanded methyl pentad region of sample 6.

As normally observed, the polymer molecular weight is lowered by adding hydrogen. Furthermore, the addition of hydrogen produces up to a 2-fold increase in productivity.[6d] This differs from literature data on heterogeneous[2] systems, where a stronger activating effect is generally reported, but is in line with what is observed for homogeneous, less regiospecific catalytic systems.[3] The fact that H_2 activates both highly regiospecific and less regiospecific zirconocene catalysts points at a common, or similar, type of deactivation process for both classes of C_2-symmetric metallocene catalysts. This aspect is discussed in part 2 of this work, where the formation and reactivation of Zr(allyl) species is analyzed.

Proton NMR analysis of the unsaturated end groups of the *i*-PP samples prepared with **1**/MAO in the presence of hydrogen shows that the main *intra*molecular chain transfer reaction is β-CH_3 elimination, while the microstructural analysis of the polymer samples by ^{13}C NMR spectroscopy revealed an unexpected result on the composition of the saturated end groups. As shown in Figure 1 and Table 2, along with the peaks of the "normal" chain-end groups (i.e., the *n*-propyl group, A, isobutyl end group, B, and traces of allyl end group, D), a new set of signals (C) appeared in the ^{13}C NMR spectra of polypropene samples.

From the quantitative analysis of ^{13}C NMR spectra (see Table 2) we can observe that, as expected, the amount of isobutyl and *n*-propyl end groups increases

(5) Busico, V.; Cipullo, R.; Corradini, P. *Makromol. Chem. Rapid Commun.* **1992**, *13*, 15.

(6) (a) Resconi, L.; Piemontesi, F.; Camurati, I.; Sudmeijer, O.; Nifant'ev, I. E.; Ivchenko, P. V.; Kuz'mina, L. G. *J. Am. Chem. Soc.* **1998**, *120*, 2308. (b) Resconi, L.; *Polym. Mater. Sci. Eng.* **1999**, *80*, 421. (c) Resconi, L.; Camurati, I.; Sudmeijer, O. *Top. Catal.* **1999**, *7*, 145. (d) Camurati, I.; Fait, A.; Piemontesi, F.; Resconi, L.; Tartarini, S. In *Advanced Catalysis: New Polymer Syntheses and Modifications*; Boffa, L. S., Novak, B. M., Eds.; Symposium Series; American Chemical Society: Washington, DC, in press.

Table 2. Quantitative Analysis of Chain-End Groups in Polypropenes Obtained with 1/MAO

Sample	p(H_2) bar	A % mol	C % mol	B % mol	D % mol	A/C	Initiating Chain-end groups C + A % mol	Terminating Chain-end groups B – D % mol
1	0	n.d.	n.d.	n.d.	n.d.	-	-	-
2	1	0.11	0.02	0.16	0.00	5.5	0.13	0.16
3	2	0.13	0.04	0.15	0.05	3.3	0.17	0.10
5	4	1.02	0.23	1.41	0.05	4.4	1.25	1.36
6	4	1.50	0.33	1.93	0.04	4.5	1.83	1.89

Scheme 1

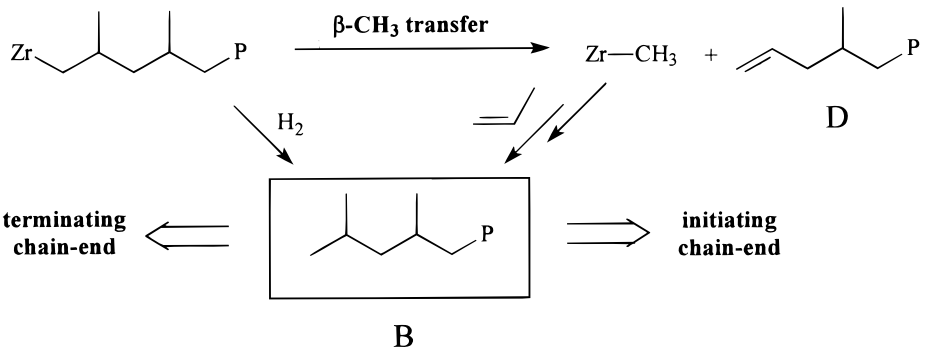

with hydrogen pressure. The same behavior can be noticed in the case of the new group (C in Table 2). Furthermore, the A/C ratio is almost constant (≈5) in samples 3−5. These facts suggest that the new group is also a chain-end.

To better understand the nature of this group, we have to make a balance between the initiating and terminating chain ends. As the chain-end B can be formed in two ways (see Scheme 1), i.e., from β-methyl transfer (it is an initiating chain-end) or from hydrogen transfer (it is a terminating chain-end), we have to split the two different contributions as $[B_{term}] = [B] - [B_{init}] = [B] - [D]$ (where B_{term} refers to the fraction of isobutyl group from hydrogen transfer, and B_{init} is the fraction from reinitiation after β-methyl transfer).

As the relation C + A ≈ B − D is verified for samples 2−6 (see Table 2), we can safely assign group C to an initiating chain-end associated with the direct insertion of propene in a Zr−H bond. The complete identification of this new chain-initiating group was performed using monodimensional (DEPT) and bidimensional (GRASP−HSQC and GRASP−HMBC) NMR techniques.[7] The more reliable structure for this chain-end group derives from a regioirregular propene insertion in the Zr−H bond followed by regio- and stereospecific propene insertions (see below) according to Scheme 2.

The same set of signals was observed by Busico and Chadwick in ^{13}C NMR spectra of some polypropenes obtained from heterogeneous systems.[8] Independently, Randall reported on a similar assignment scheme in the case of propene polymerization by using less regiospecific metallocenes in the presence of hydrogen.[9]

Scheme 2

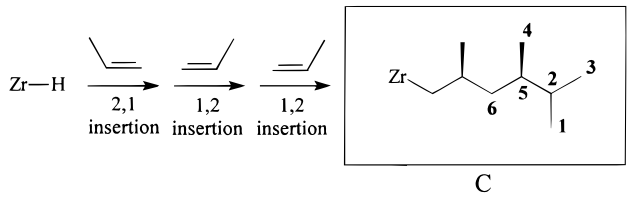

Table 3. ^{13}C and ^{1}H NMR Assignments

position[a]	type	chemical shift (ppm) carbon	chemical shift (ppm) hydrogen
1	CH_3	17.76	0.89
2	CH	31.93	1.67
3	CH_3	20.56	0.96
4	CH_3	16.30	0.89
5	CH	36.47	1.51
6	CH_2	43.05	0.93/1.42

[a] See atom numbering in Scheme 2

The complete ^{1}H and ^{13}C NMR assignments are reported in Table 3. The chemical shift difference of the two diastereotopic hydrogen atoms on carbon 6 ($\Delta\delta$ = 0.49 ppm) can help us to assign the relative configuration of the two nearest methines. In fact, by comparing our value with the values found by Mizuno[10] for a similar CH_2 group next to a 2,1-*erythro* (CH_2 in a *meso* dyad) or a 2,1-*threo* (CH_2 in a *racemic* dyad) regioirregular propene unit (see Scheme 3), it is evident that in group C the CH_2 is in a *meso* dyad. This indicates a highly stereospecific propene insertion after the initial regio mistake.

With the aim of rationalizing the above experimental evidence that a large fraction (about 20%) of propene

(7) (a) Bendall, M. R.; Doddrell, D. M.; Pegg, D. T. *J. Am. Chem. Soc.* **1981**, *103*, 4603. (b) Schenker, K. V.; v. Philipsborn, W. *J. Magn. Reson.* **1986**, *66*, 219. (c) Kay, L. E.; Keifer, P.; Saarinen, T. *J. Am. Chem. Soc.* **1992**, *114*, 10663. (d) Kay, L. E.; Keifer, P.; Saarinen, T. *J. Am. Chem. Soc.* **1992**, *114*, 10663.

(8) Busico, V.; Chadwick, J. C. Personal communication.

(9) Randall, J. C.; Ruff, C. J.; Vizzini, J. C.; Speca, A. N.; Burkhardt, T. J. In *Metalorganic Catalysts for Synthesis and Polymerisation*; Kaminsky, W., Ed.; Springer-Verlag: Berlin, 1999; p 601.

(10) Mizuno, A., Tsutsui, T.; Kashiwa, N. *Polymer* **1992**, *33*, 254.

Scheme 3

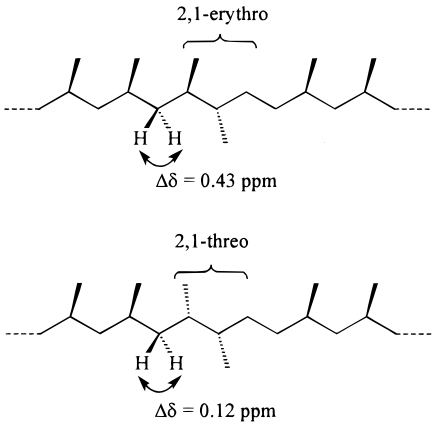

insertions on the [*rac*-Me_2C(3-*t*-Bu-1-Ind)$_2$Zr−H]$^+$ species proceeds in a *secondary* fashion, a DFT quantum mechanics/molecular mechanics study (see computational details) on the evolution of the analogous [H_2C(3-*t*-Bu-1-Ind)$_2$Zr−H]$^+$/propene system has been performed.[11] This approach has been successfully employed in a number of theoretical studies and is based on the assumption that the core of the molecular system (that is the active site, at which processes of bond breaking and forming take place) must be described by an electronic structure calculation, while the rest of the system (perturbating the active site only through steric hindrance) can be described by the simpler (and computationally faster) molecular mechanics treatment.

Theoretical Investigation on the Evolution of the Zr−H Species. A metal−hydride bond is generated upon chain-transfer reaction with molecular hydrogen. This highly unsatured species has a strong tendency to react with a new monomer molecule: test calculations show that the olefin in the [L_2ZrH(propene)]$^+$ complex (where L_2 = (*R*,*R*)-H_2C(3-*t*-Bu-1-Ind)$_2$) has a coordination energy of nearly 30 kcal/mol. We are aware that our model is largely approximated: in fact, the system is considered in vacuo, and moreover, the presence of a counterion, as well as the influence of entropic factors, is neglected. However, Ziegler and co-workers have recently given good reasons for neglecting the influence of the counterion and also reported that the $T\Delta S$ value for ethylene uptake is about −10 kcal/mol.[12a,b] Therefore, we can reasonably assume that coordination of a propene molecule on the [L_2Zr−H]$^+$ species is a largely favored and possibly nonactivated process, even though its exothermicity could be overestimated.

In principle, a propene molecule can coordinate to the Zr−H species in four ways: primary (1,2) and secondary (2,1), both with either *re* or *si* enantiofaces. The optimized structures of the [L_2Zr−H(propene)]$^+$ species in which the monomer molecule is 1,2-*re* (model **1a**) and 1,2-*si* coordinated (model **1b**) are shown in Figure 2. In the same figure, model **1c** shows the optimized structure of [L_2Zr−H(propene)]$^+$ with a coordinated 2,1-*si* propene. All attempts at optimizing the structure including a 2,1-*re* propene inexorably led to the 2,1 insertion product [L_2Zr(isopropyl)]$^+$ (model **2b** in Figure 2). As a possible rationalization of this behavior, we recall that the enantioselectivity of the regioirregular propene insertions into a growing polypropene chain was explained in terms of nonbonded interactions between the ligand and the methyl group of propene.[13] It was shown that in models with an (*R*,*R*)-*ansa*-π-ligand, the coordination of a *secondary* 2,1-*re* monomer is disfavored by repulsive interaction with the ligand (see Figure 4 in ref 13): similarly, geometries in which the growing chain is replaced by a H atom show small nonbonding distances between the methyl group of a coordinating 2,1-*re* propene and one six-membered ring of the ligand. As a consequence, the olefin is "pushed" to insert into the Zr−H bond, giving rise to the more compact Zr(isopropyl) insertion product **2b**. In Table 4, a splitting of the energy differences in terms of their quantum mechanics and molecular mechanics components for all the species considered in this work is reported. For the Zr−H(propene) complexes, the most stable structure corresponds to the *secondary si* propene coordination (model **1c**). This effect is electronic in nature and is due to an agostic bond between the metal and one of the hydrogen atoms of the methyl group of propene, whereas this interaction is not allowed in models (**1a** and **1b**) for *primary* monomer coordinations. The occurrence of this agostic interaction in models including a propene molecule 2,1 coordinated to Zr−H was first reported by Prosenc and Brintzinger in a modelistic study on the isomerization process of the *n*-propyl growing chain on the [$Cp_2ZrC_3H_7$]$^+$ species.[14]

Insertion into the Zr−H Bond. Some authors have already investigated the process of hydrogen transfer to the metal center from *n*-propyl units[14−16] and the insertion of coordinated 2,1 propene into the Zr−H bond to give an isopropyl unit.[14,16] Since there is a substantial agreement between the energy barriers shown in the mentioned studies (particularly with those of ref 14) and our results, we just summarize our findings in Table 4 and recall that both primary and secondary insertions occur with small activation barriers (less than 1 kcal/mol). In the Zr(isopropyl) complex, both the isopropyl methyls show an agostic interaction with the zirconium and are located at nearly the same distance to the metal center (see different views of **2b** in Figures 2 and 7).[17] This conformation provides the best interaction with the low-lying metal-centered LUMOs localized in the "equatorial" plane between the Cp ligands.[18] Figure 3 depicts the relative energy along the two possible "primary" and "secondary" pathways representing the evolution of the [L_2Zr−H]$^+$/propene system: since the reactive Zr−H species always reacts with the monomer with small activation barriers, primary and secondary propene

(11) Computations have been performed on (*R*,*R*)-H_2C(3-*t*-Bu-Ind)$_2$ for simplicity. Actually, *rac*-H_2C(3-*t*-Bu-Ind)$_2ZrCl_2$ is a real and improved version of **1** that maintains all features typical of **1**/MAO. Indeed, test calculations with the (*R*,*R*)-Me_2C(3-*t*-Bu-Ind)$_2$ ligand gave quite comparable results; for details, see: Resconi, L.; Balboni, D.; Dang, V. A.; Yu, L. C. PCT WO 98/43989. Resconi, L.; Balboni, D.; Baruzzi, G.; Fiori, C.; Guidotti, S. Submitted to *Organometallics*.

(12) Deng, L.; Ziegler, T.; Woo, T. K.; Margl, P.; Fan, L. *Organometallics* **1998**, *17*, 3240. (b) Moscardi G.; Woo, T. K.; Deng, L.; Ziegler, T. *A Combined DFT QM/MM Study on the Associative Displacement of the Terminated Polymer Chain in Ni(II) Diimine-Catalyzed Ethylene Polymerization*. Unpublished work.

(13) Guerra, G.; Cavallo, L.; Moscardi, G.; Vacatello, M.; Corradini, P. *J. Am. Chem. Soc.* **1994**, *116*, 2988.

(14) Prosenc, M. H.; Brintzinger, H. H. *Organometallics* **1997**, *16*, 3889.

(15) Yoshida, T.; Koga, N.; Morokuma, K. *Organometallics* **1995**, *14*, 746.

(16) Thorsaug, K.; Støvneng J. A.; Rytter, E.; Ystenes, M. *Macromolecules* **1998**, *31*, 7149.

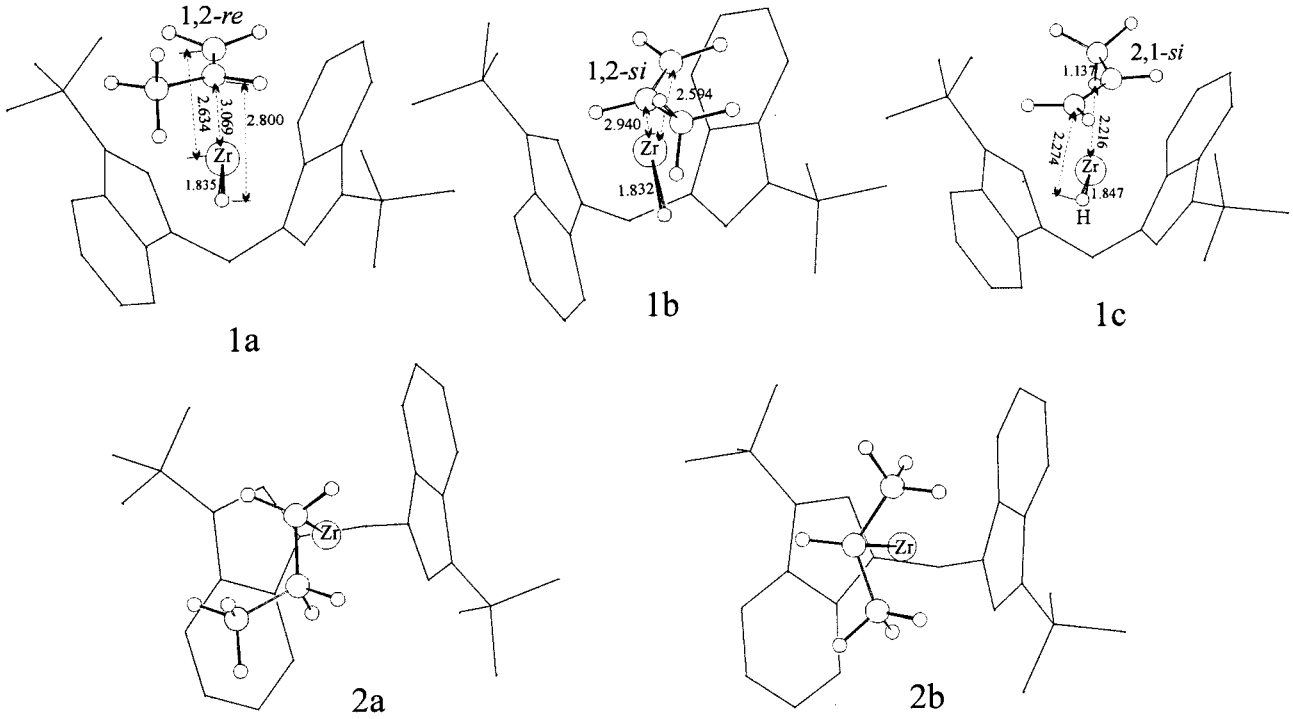

Figure 2. Models for propene coordination on the $[L_2Zr-H]^+$ complex in which the aromatic ligand is (*R*,*R*) coordinated to the metal and related insertion products. Hydrogen atoms on the ligand framework have been omitted for clarity.

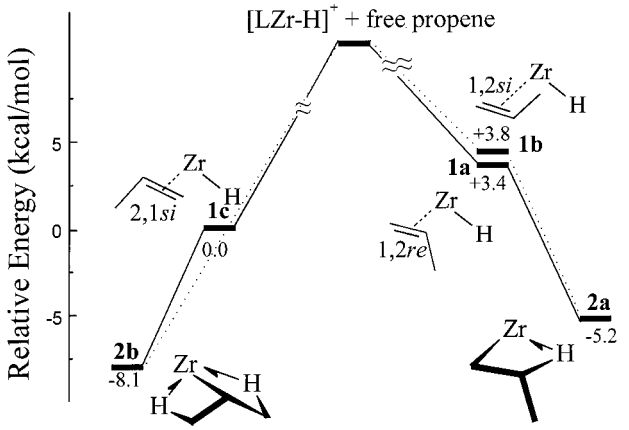

Figure 3. Reaction between cationic hydride complex and propene leading to the formation of *n*-propyl and isopropyl units. Solid and dotted lines refer to processes in which *si* and *re* propene are involved, respectively. Insertion barriers are not shown.

insertions should have the same probability. This result does not agree with our experimental data, which clearly indicate that the majority (≈80%) of the initiating groups are *n*-propyl (Table 2). In the following, we will show that the way the isopropyl interacts with the metal has a detrimental effect on the propagation reaction and will provide a rationalization for the "dormancy" of the catalytic site bearing an isopropyl group.

Table 4. Relative Energies (kcal/mol) of the Species Involved in the Studied Processes

	Δ*E*(Tot)	Δ*E*(QM)	Δ*E*(MM)
Zr−H(propene) Complexes[a]			
1c	0.0	0.0	0.0
1a	3.4	3.4	0.0
1b	3.8	3.6	0.2
Propene Insertion into Zr−H[a]			
TS[1a−2a]	+3.5	+3.4	+0.1
2a	−5.2	−5.4	0.2
TS[1c−2b]	0.3	−0.2	0.5
2b	−8.1	−8.2	0.1
Propene Insertion into Zr(*n*-propyl)[b]			
3a	−10.3	−10.9	0.6
max[3a→3b]	−6.1	−7.0	0.9
3b	−10.1	−10.5	0.4
4a	−9.8	−9.5	−0.3
insertion product	−20.5	−19.0	−1.5
Propene Insertion into Zr(isopropyl) [c]			
TS[2b−2c]	9.0	8.3	0.7
2c	5.9	5.7	0.2
3c	−5.3	−6.6	1.3
4b	−1.0	−1.6	0.6
insertion product	−15.9	−14.4	−1.5
Propene Rotation in the Two-Step Isomerization[a]			
5a	8.1	8.6	−0.5
5b	8.0	9.2	−1.2
Displacement of 2,1 Propene from **1c**[a]			
6	−8.3	−7.9	−0.4

[a] Energy of **1c** chosen as reference value. [b] Energy of **2a** chosen as reference value. [c] Energy of **2b** chosen as reference value.

Comparative Study on the Propagation Step for Catalytic Sites Bearing a *n*-Propyl and Isopropyl Chain. Propene Insertion into Zr(*n*-propyl). The

(17) As a main difference with calculations of refs 14 and 16, we find that the 2,1 insertion product—the Zr(isopropyl) species **2b**—is more stable than Zr(*n*-propyl) **2a**. To check to what extent our findings depend on both the particular ligand and the computational technique, we compared the relative stability and the geometric features of the [Ligand Zr(*n*-propyl)]$^+$ and [Ligand Zr(isopropyl)]$^+$ complexes (Ligand = Cp_2, $H_2C(Cp)_2$, *rac*-[H_2C(1-Ind)$_2$]): while for Ligand = Cp_2 we reproduced the results shown in refs 14 and 16; with all the bridged ligands we again found a higher stability of the Zr(isopropyl) species. In our opinion, this is due to the more open ligand geometry induced by the bridge: in fact, while for the Cp_2 the angle between the mean planes of the five-membered rings is about 50°, for all the bridged ligands this value is more than 70°. Evidently, repulsive steric interactions in the unbridged catalysts disfavor the more electronically stable Zr(isopropyl) species.

(18) Lauher, J. W.; Hoffmann, R. *J. Am. Chem. Soc.* **1976**, *98*, 1729.

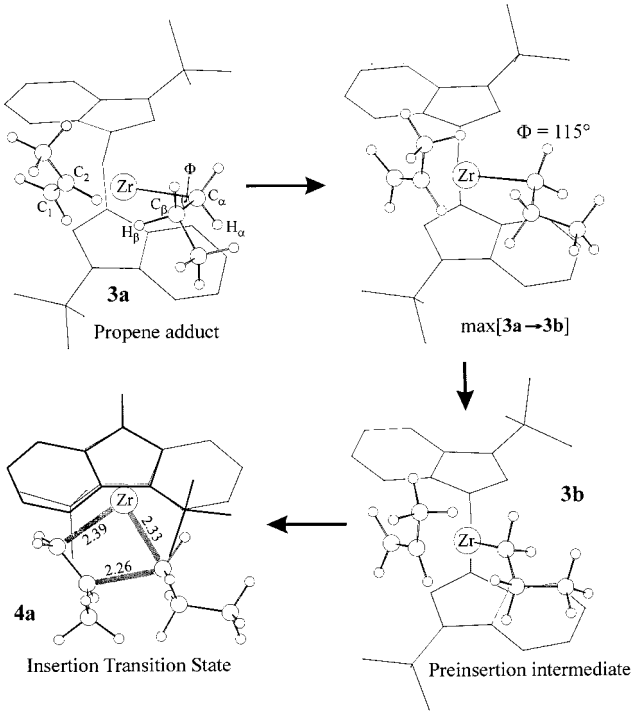

Figure 4. Concerted propene coordination−chain rearrangement process for the formation of the preinsertion intermediate (**3b**) starting from the olefin adduct (**3a**) and transition state for propene insertion into the Zr−C_3H_7 bond (**4a**). The hydrogen atoms on the ligand framework have been omitted for clarity. Thicker lines represent bonds above the plane of the paper.

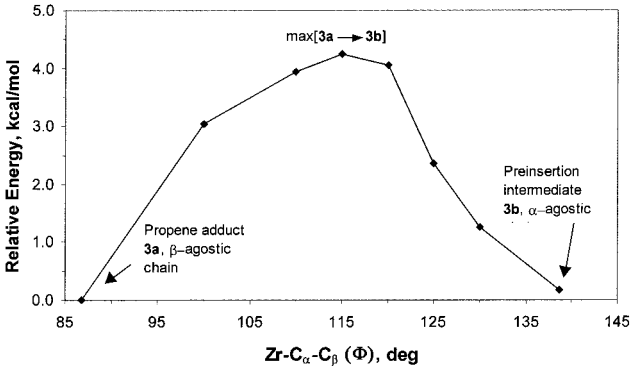

Figure 5. Energy profile for the concerted propene coordination−chain rearrangement process from **3a** to **3b**.

ethylene insertion step onto a linear growing chain has been investigated in several theoretical works.[15,16,19,20] In particular, the insertion of ethylene in the presence of the bisCp and bis(Me_5Cp) ligands has been among the subjects of ref 16, in which the authors also investigated the process of chain propagation starting from a γ-agostic *n*-propyl. However, other authors evidenced that the direct precursor to olefin insertion is the chain with a β-agostic bond, since γ-agostic bonds are replaced by β-agostic ones prior to insertion.[20] Moreover, calculations aimed at optimizing a structure in which a *si*-propene, a γ-agostic isobutyl chain, and a

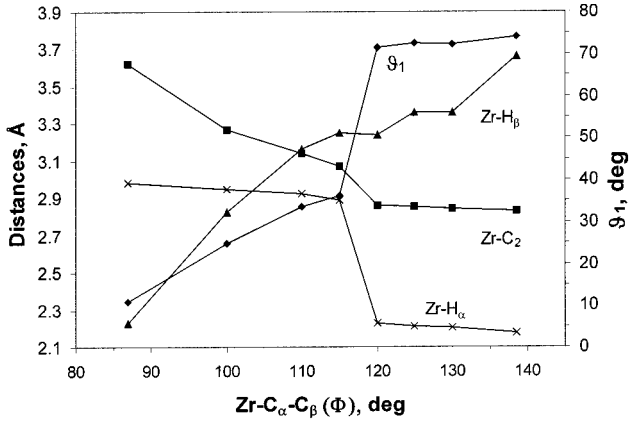

Figure 6. Geometric aspects of the concerted chain rearrangement−monomer coordination processes leading to the formation of the preinsertion intermediate for the primary (1,2) monomer insertion.

(*R*,*R*)-Me_2C(3-*t*-Bu-Ind)$_2$ ligand are bonded to a zirconium center resulted in the formation of the β-agostic isobutyl, *si*-propene π-complex.[21] Therefore, we chose not to further investigate the alternative insertion route proceeding from the γ-agostic conformation of the *n*-propyl.

Experimental data show that monomer insertion into both *n*-propyl and isopropyl initiating groups is primary and occurs with the same preferred enantioface of the successive insertion steps. Moreover, as already pointed out in a recent molecular mechanics study by some of us,[22] the *si* enantioface has been found to be the "right" one for (*R*,*R*)-Me_2Si(3-*t*-Bu-1-Ind)$_2Zr Cl_2$. Therefore, we have restricted our study to the primary *si*-propene propagation starting from the β-agostic structure **2a** in the presence of the sterically crowded ligand framework provided by the (*R*,*R*)-[H_2C(3-*t*-Bu-Ind)$_2$]$ZrCl_2$ catalyst.

In the presence of the sterically unhindered bis(cyclopentadienyl) ligand, the formation of a π-bonded ethylene, β-agostic *n*-propyl complex as a precursor for chain propagation has been found by Rytter et al. to proceed without energy barrier.[16] The same authors found that to form an analogous complex in models including the crowded bis(pentamethylcyclopentadienyl) ligand, an ethylene molecule has to be "pushed" into the ligand framework, overcoming an energy barrier of nearly 9 kcal/mol. Our attempts to optimize the structure of a zirconocene model complex with the [H_2C(3-*t*-Bu-1-Ind)$_2$] ligand, a *n*-propyl β-agostic chain, and a π-coordinated *si*-propene without any geometry constraint led to the formation of an adduct (labeled **3a** in Figure 4) which is stabilized by nearly 10 kcal/mol with respect to the β-agostic complex **2a** plus free propene system. This complexation enthalpy is considered sufficiently exothermic to guarantee a good catalytic activity.[23] Then, the rearrangement of the growing chain toward the α-agostic conformation and olefin coordination to form a preinsertion intermediate (**3b** in Figure 4) proceeds in our opinion in a concerted fashion. In Figures 5 and 6, the relative energy and the variation of several geometrical parameters as Zr−C_2, Zr−H_α, and

(19) Lohrenz, J. C. W.; Woo, T. K.; Ziegler, T. *J. Am. Chem. Soc.* **1995**, *117*, 12793.
(20) Woo, T. K.; Margl, P. M.; Lohrenz, C W.; Blöchl, P. E.; Ziegler, T. *J. Am. Chem. Soc.* **1996**, *118*, 13021.
(21) Resconi, L. Fait, A.; Piemontesi, F.; Camurati, I.; Moscardi, G.; Cavallo, L.; Milano, G. Part 2 of this work, manuscript in preparation.
(22) Toto, M.; Cavallo, L.; Corradini, P.; Moscardi, G.; Resconi, L.; Guerra, G. *Macromolecules* **1998**, *31*, 3431.
(23) Margl, P.; Deng, L.; Ziegler, T.*Organometallics* **1998**, *17*, 933.

Scheme 4

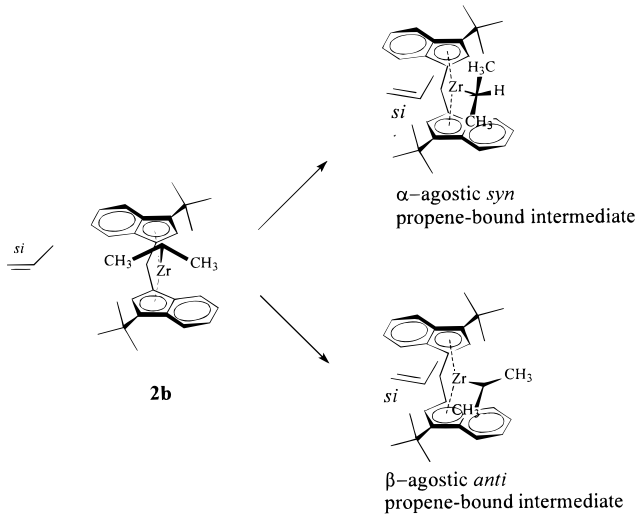

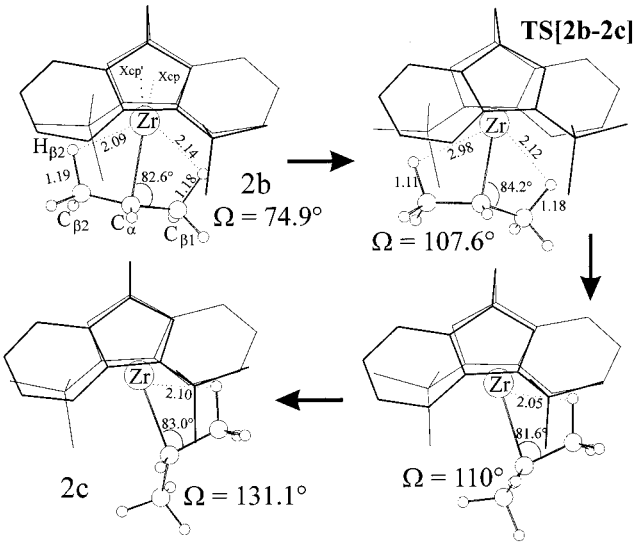

Figure 7. Rearrangement of the isopropyl group from the double to the single β-agostic conformer. Thicker lines represent bonds above the plane of the paper. Ligand hydrogens are omitted for clarity. Ω is the improper torsion angle $Zr-C_{\beta1}-C_{\alpha}-C_{\beta2}$. Xcp and Xcp′ indicate the centroids of the five-membered rings.

$Zr-H_{\beta}$ distances (atom labeling: see **3a** in Figure 4) and the dihedral angle $C_1-Zr-C_{\alpha}-C_{\beta}$ (labeled ϑ_1) are depicted versus the $Zr-C_{\alpha}-C_{\beta}$ angle (in the following labeled as Φ), which has been found to be the best reaction coordinate.[16] The β-agostic bond is almost completely lost at $\Phi = 100°$, but due to repulsive interactions between the chain and the monomer, the π-complex cannot be completely established. Moreover, the chain conformation is not yet suitable for an α-agostic interaction. Only at $\Phi = 120°$ is the formation of a π-olefin, α-agostic complex allowed, as one can see from the sudden variation of ϑ_1 and the other relevant distances. Further opening of Φ only reduces the steric repulsions between monomer and chain, but geometric parameters do not change significantly. Starting from the preinsertion intermediate **3b**, the decrease of the C_2-C_{α} distance gives rise to the γ-agostic insertion product. Model **4a** in Figure 4 depicts the transition state for monomer insertion. Its energy is only 0.30 kcal/mol above that of the preinsertion intermediate **3b**. Summing up, the β-agostic → α-agostic rearrangement process in concert with monomer coordination is the rate-determining step for propagation. The calculated energy barrier (4.2 kcal/mol, obtained as the difference between the energy level of max[**3a**→**3b**] and that of **3a** in Table 4) is similar to that found in analogous calculations performed on the (*R*,*R*)-[Me_2C(3-*t*-Bu-1-Ind)$_2$Zr(*si*-propene)(isobutyl)]$^+$ model.[21]

Propene Insertion into Zr(isopropyl). Propene insertion can start from an alkene-bound state in which the isopropyl can be either α-agostic or β-agostic (see Scheme 4). In the former, the methyl group of the propene is *syn* (i.e., close) to one methyl of the isopropyl, while in the β-agostic geometry these groups are in an *anti* disposition. A comparison by molecular mechanics calculations[22,24] between approximate transition states for propene insertion into a primary growing chain in which the propene methyl group and the chain are *syn* and *anti*, respectively, indicated that the *syn* transition state is 3−5 kcal/mol higher in energy. Therefore, we assume that the propene insertion into the Zr(isopropyl) species with an α-agostic interaction is disfavored and restrict our investigation to the insertion step into the β-agostic conformer of the $[L_2Zr(isopropyl)]^+$ species.

As remarked before, our models do not represent the *real* system: in particular, the presence of a high amount of monomer (polymerization tests were performed in *liquid* monomer) is not accounted for. However, our goal is not to evaluate the energy stabilization of metal complexes due to interactions with surrounding monomer (which, in principle, can take place for all the considered models), but to verify whether the monomer has a role into a specific reaction of the catalytic cycle. In the previous section, we have shown that the rearrangement of chain conformation (from β- to α-agostic) and monomer coordination could be concerted processes starting from an olefin adduct. The insertion reaction into the Zr(isopropyl) bond has been investigated by looking for an analogous concerted channel; however, the conformation of the isopropyl (as discussed above) in the alkene-free state causes the monomer coordination step to be quite different. The high stability of the $[L_2Zr(isopropyl)]^+$ species and the strong nonbonded interactions between the olefin and the closest methyl group of the isopropyl prevent the formation of a catalyst−propene adduct; in fact, all attempts to optimize such a structure without geometry costraints always resulted in the rejection of the monomer ($Zr-C_{olefin} > 5$ Å). This suggests that the propagation reaction probably proceeds through a rearrangement of the isopropyl in order to make room for the incoming monomer. Indeed, we investigated such a process by choosing as a reaction coordinate the improper torsional angle $Zr-C_{\beta1}-C_{\alpha}-C_{\beta2}$ [16] (labeled Ω, see model **2b** in Figure 7 for atom labeling). Some optimized structures calculated for the rearrangement step are shown Figure 7; it is worth noting that initially the isopropyl tends to keep its symmetrical conformation. Only at $\Omega \approx 110°$ does a sudden shift toward a different conformation occur, as one can see also on inspection of models in Figure 7 and from the plots of Figures 8 and 9, in which the trends of the relative energy and of some relevant

(24) Kawamura-Kuribayashi, H.; Koga, N.; Morokuma, K. *J. Am. Chem. Soc.* **1992**, *114*, 8687.

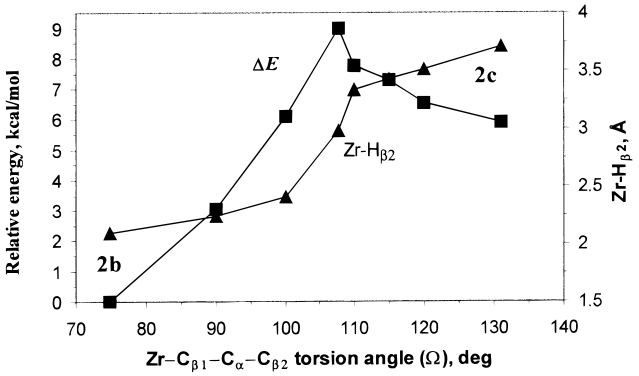

Figure 8. Energy profile for the rearrangement of the Zr-(isopropyl) from **2b** to **2c** (see Figure 7 for atom labeling).

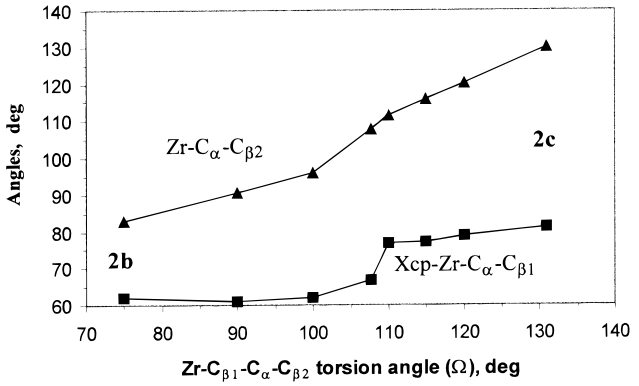

Figure 9. Geometric aspects of the unimolecular rearrangement of Zr(isopropyl) from **2b** to **2c** (see Figure 7 for atom labeling).

geometric parameters are reported for the conversion of **2b** into **2c**. Test calculations aimed at finding a stable olefin π-complex at $\Omega = 100°$ and 110° confirm that the monomer does not take part in the isopropyl rearrangement process until a conformer with a *single* β-agostic interaction of the isopropyl (**2c,** in which ϑ is nearly 130°) is formed. In fact, we find that at $\Omega = 110°$ the olefin carbons are still at nearly 5 Å from the metal. The energy profile of Figure 8 shows that the loss of the agostic interaction between one of the β-hydrogens with the metal center passes over an energy barrier of 9.0 kcal/mol. The single β-agostic species **2c** is able to coordinate a monomer, leading to the formation of the preinsertion intermediate **3c** shown in Figure 10. The insertion step then follows the known C_2-C_α reaction coordinate, with an activation energy of 4.4 kcal/mol (see Table 4 and model **4b** in Figure 10), leading to a δ-agostic insertion product. The propagation into the Zr-(isopropyl) bond looks similar to the so-called "backside insertion" already discussed in various papers for the polymerization of ethylene.[16,19,20] In particular, Ziegler and co-workers evidenced in ref 19 the influence of entropic effects, which can further disfavor this process in zirconocene catalysts. Therefore, the activation barrier for monomer insertion into the Zr(isopropyl) bond could be underestimated.

Ratio between "Initiating" Groups. Figure 11 summarizes our results on the evolution of the $[L_2Zr-H]^+$/propene system, proceeding from the first monomer insertion into the Zr−H bond to the successive one. By comparing the path after the initial 2,1 propene insertion into the Zr−H bond with the one that follows the

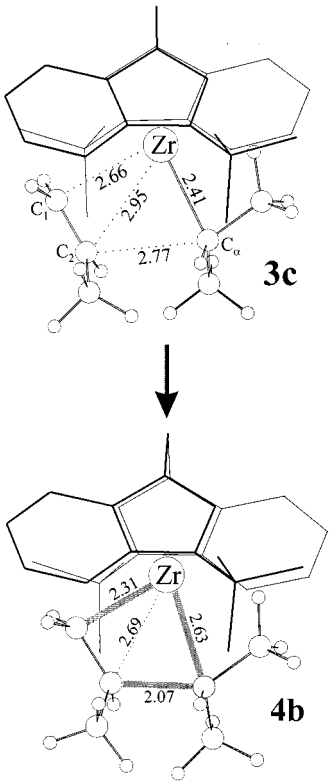

Figure 10. Preinsertion intermediate **3c** and the transition state **4b** for propene insertion into the Zr(isopropyl) bond. Thicker lines represent bonds above the plane of the paper. Ligand hydrogens omitted for clarity.

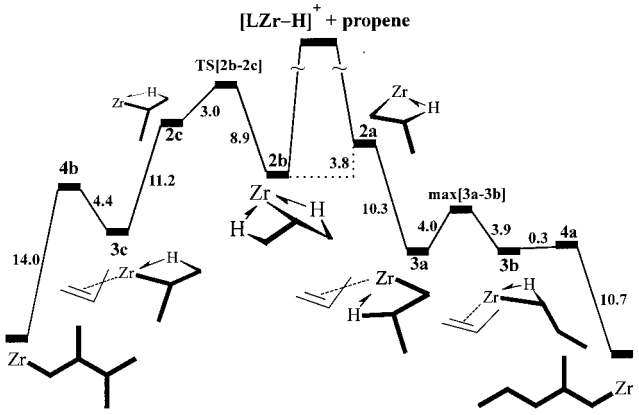

Figure 11. Schematic reaction profiles for propene insertion into Zr−H and Zr−alkyl bonds. Energy differences in kcal/mol.

initial 1,2, it is evident that catalytic sites bearing *n*-propyl and isopropyl groups do have much different propagation barriers.

In particular, the formation of the olefin adduct **3a** starting from Zr−H and free propene does not have a significant activation barrier, further indicating that 1,2 propene insertion into Zr−H is irreversible. On the contrary, the Zr(isopropyl) species **2b** must rearrange to a less stable conformer **2c** before reacting with the monomer. The "dormant" nature of **2b** can prevent the formation of a nearly equal number of "initiating" *n*-propyl and isopropyl groups (as the results on the insertion into Zr−H could suggest) if the "slow" site undergoes side reactions. As shown in Scheme 5, in the

Scheme 5

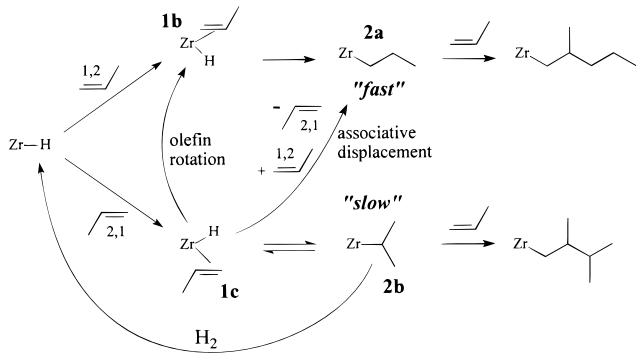

presence of hydrogen the Zr(isopropyl) species could be decomposed in propane and a Zr−H species. Other options arise form the evidence that the "slow" site **2b** can propagate through rearrangement into **2c** or undergo hydride transfer back to **1c** with comparable energy barriers (that is, the 2,1 propene insertion into the Zr−H bond is reversible). We now analyze the possible mechanisms for the **2b** → **2a** isomerization. In principle, this can occur in three different ways (excluding unimolecular β-H transfer to Zr and dissociation of the 2,1 propene): (1) bimolecular β-H transfer to the monomer; this mechanism can be ruled out by the fact, outlined in the previous section, that the rearrangment of **2b** generates the "backside" monomer coordination (that is, propene *anti* to the β-agostic bond, see Figures 7 and 10), which is not a suitable precursor of a bimolecular hydrogen exchange process; (2) β-H transfer to Zr, rotation from secondary to primary of the coordinated propene, then reinsertion into the Zr−H bond; (3) β-H transfer to Zr and associative displacement by a new monomer molecule. We have tested these last two alternatives.

Direct Isomerization. The simplest hypothesis for a mechanism that changes a 2,1-coordinated α-olefin into a primary (1,2) one is in-plane rotation.[14,16] This process is part of the two-step mechanism proposed by Chien[25] for the 2,1 → 3,1 isomerization of the secondary growing chain-end, which has been observed in poor regiospecific zirconocenes.[25−29] In this section, we briefly investigate the influence of the $[H_2C(3\text{-}t\text{-Bu-1-Ind})_2]$ ligand framework, which is both bridged and C_2 symmetric, on the energetics of propene rotation that shifts the $[L_2Zr{-}H(2,1\text{-propene})]^+$ species (**1c**) into the $[L_2Zr{-}H(1,2\text{-propene})]^+$ one (**1b**). In Figure 12, the total QM/MM energy is plotted as a function of the H−Zr−X_{ol}−C_1 dihedral angle (labeled ϑ_0; X_{ol} indicates the centroid of the propene double bond, see Figure 13 for atom labeling), while in Figure 13 are shown the structures **5a** and **5b**, corresponding to the two maximums of the rotation path. The strong nonbonded interactions between the rotating propene and the ligand force the olefin to interact with the metal in a highly unsymmetrical fashion. It is our feeling that in this situation of high energy the rotating olefin could be easily displaced by a new monomer molecule. To our knowledge, only Prosenc and Brintzinger have so far proposed a mechanism that is alternative to in-plane olefin rotation.[14]

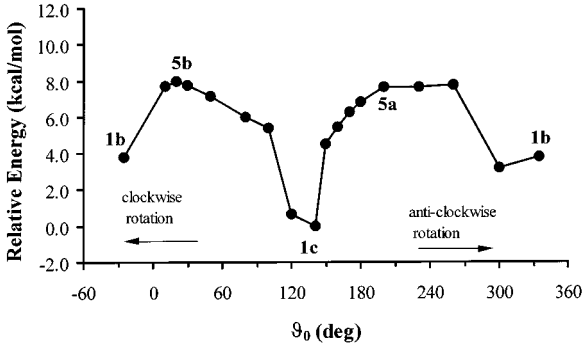

Figure 12. Energy profile for the step of propene rotation (with respect to the H−Zr−X_{ol}−C_2 dihedral angle) in the two-step isomerization mechanism.

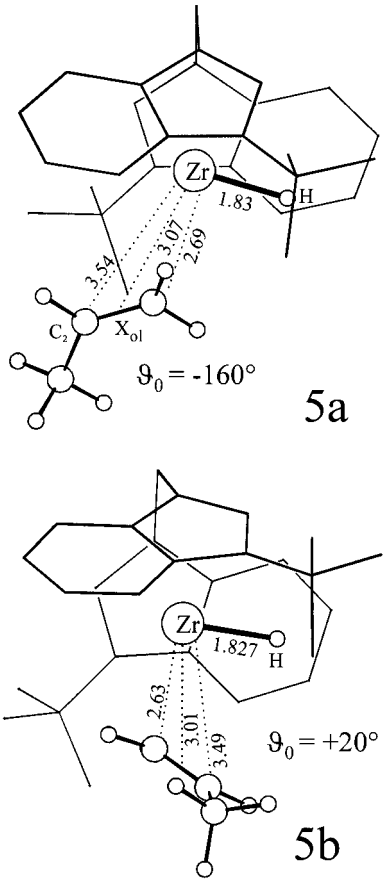

Figure 13. Selected geometries corresponding to points **5a** and **5b** of Figure 12. Thicker lines represent bonds above the plane of the paper. Ligand hydrogens are omitted for clarity.

Associative Displacement. The reaction between the $[L_2Zr{-}H(2,1\text{-propene})]^+$ species (**1c**) and a *primary* propene could either reverse the hydrogen-transfer process back to the "dormant" species $[L_2Zr(\text{isopropyl})]^+$ (**2b**) or, alternatively, generate the $[L_2Zr(n\text{-propyl})]^+$ complex upon *primary* propene insertion into the Zr−H bond with concurrent dissociation of the *secondary* propene, that is, insertion by associative displacement of the 2,1 propene.[30] This latter hypothesis is supported

(25) Rieger, B.; Chien, J. *Polym. Bull.* **1989**, *21*, 159.
(26) Resconi, L.; Fait, A.; Piemontesi, F.; Colonnesi, M.; Rychlicki, H.; Zeigler, R. *Macromolecules* **1995**, *28*, 6667.
(27) Busico, V.; Caporaso, L.; Cipullo, R.; Landriani, L.; Angelini, G.; Margonelli, A.; Segre, A. L. *J. Am. Chem. Soc.* **1996**, *118*, 2105.
(28) Soga, K.; Shiono, T.; Takemura, S.; Kaminsky, W. *Makromol. Chem., Rapid Commun.* **1987**, *8*, 305.
(29) Schupfner, G.; Kaminsky, W. *J. Mol. Catal. A: Chem.* **1995**, *102*, 59.
(30) Johnson, L. K.; Killian, C. M.; Brookhart, M. *J. Am. Chem. Soc.* **1995**, *117*, 6414.

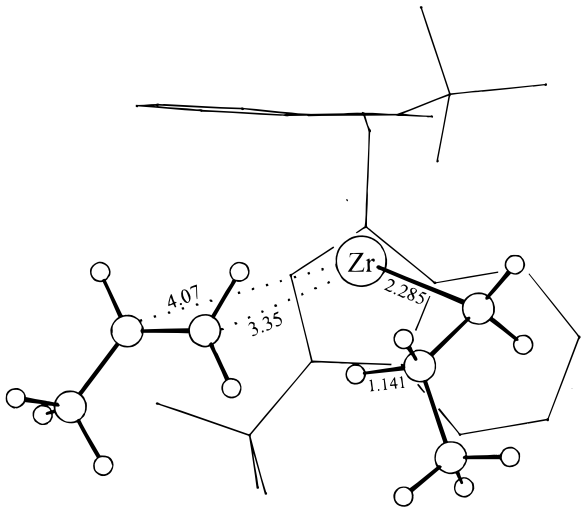

6

Figure 14. Reaction product between free propene and complex **1c** in the displacement of the 2,1-coordinated monomer. Ligand hydrogens are omitted for clarity.

by the extremely high regiospecificity of the catalyst, which suggests that in the presence of a growing chain the coordination of a 2,1 propene is highly disfavored. In other words, by this sequence of events, a bimolecular self-correcting isopropyl to *n*-propyl isomerization process occurs. To determine the energetic cost of the approach of the 1,2 propene to the inner coordination sphere of the metal, we tried to optimize a structure for a double olefin metal−hydride intermediate in which the Zr−H bond is placed between a 1,2-*si* and a 2,1-*si* propene molecule. Every attempt always resulted in the formation of the $[L_2Zr(n\text{-propyl})(2,1\text{-propene})]^+$ complex (model **6** in Figure 14). Moreover, the exothermicity (13.5 kcal/mol) of the process from **1c** plus free propene to **6** is higher than the $T\Delta S$ at room temperature for olefin uptake (about 10 kcal/mol,[12a,b]). The above results indicate that the overall process **1c** + 1,2-propene → **6** could have a fairly small activation energy. In complex **6**, the 2,1 propene is loosely bonded, and most importantly, there is no chance for its insertion into the Zr-(*n*-propyl) bond. We evaluate that in model **6** the coordination energy of the 2,1 propene is nearly 8 kcal/mol: therefore, the complete dissociation of the 2,1 propene may be a spontaneous process, since the $T\Delta S$ at room temperature for olefin dissociation is about 10 kcal/mol.[12a,b]

The results of the two proposed schemes for the conversion of 2,1 units into 1,2 ones are summarized in Figure 15: the energy barrier for the two-step isomerization (nearly 16 kcal/mol) starting from the double β-agostic species **2b** indicates that this process could be largely disfavored and that conversion of "slow" into "fast" sites (Scheme 5) could be due to hydrogen or, alternatively, to a process that reverses the initial 2,1 propene insertion, followed by the displacement of the 2,1 propene by a new 1,2 coordinating monomer.

That a self-correcting isopropyl to *n*-propyl isomerization process can also occur without hydrogenolysis is indicated also by the fact that the 2,3-dimethylbutyl group is never observed in *i*-PP samples prepared with **1**/MAO without hydrogen, even at the lowest propene concentrations, where Zr−H bonds are generated by unimolecular chain transfer to the metal.[6b−d] As a final remark, the substantial equivalence between the energy barrier for chain propagation and for 2,1 propene elimination from **1c** (Figure 15) suggests a [1,2]/[2,1] ratio of about 3, in the absence of hydrogenolysis.

Conclusions

Addition of molecular hydrogen to the polymerization of liquid propene catalyzed by *rac*-[Me_2C(3-*t*-Bu-1-Ind)-$ZrCl_2$]/MAO produces a relatively small increase in catalytic activity, while the polymer molecular weight is strongly reduced: polypropene number average molecular weight decreases from about 40 000 without hydrogen to about 2000 when $P(H_2) = 4$ bar.

A new saturated chain-end group is observed in the ^{13}C NMR spectra of these samples, which we assign to secondary propene insertion into the Zr−H bond, generated after chain transfer to hydrogen. The ratio between primary to secondary initial insertions ([1,2]/[2,1]) was found to be nearly equal to 5 and constant over the investigated range of hydrogen partial pressure.

After the initial insertion the catalyst becomes regiospecific again, as no 2,1 units inside the polymer chain are detectable in the ^{13}C NMR spectra.

Theoretical calculations provide an explanation for the observed ratio between "initiating" polypropene end groups in terms of the lower reactivity of the Zr-(isopropyl) site compared to that of the Zr(*n*-propyl)

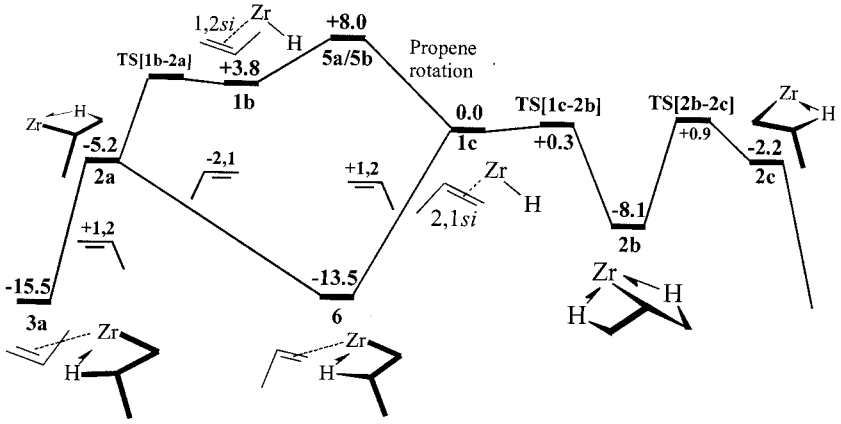

Figure 15. Schematic representation of the proposed mechanisms for the conversion of the "slow" Zr(isopropyl) site into the "fast" Zr(*n*-propyl) one. Relative energies in kcal/mol.

one: the less reactive Zr(isopropyl) undergoes competing chain-transfer reactions. As the theoretical results on the evolution of the $[L_2Zr-H]^+$ in the presence of propene have been obtained for a highly crowded model catalytic system, we believe that the same reactions can occur in less hindered catalysts, and therefore *this behavior should not be limited to the present catalytic system*. Indeed, experimental observations are accumulating that show the occurrence of 2,1 propene insertion into the Zr−H bond for both homogeneous[9] and heterogeneous[8] Ziegler−Natta catalysts.

The "dormancy" of the $[L_2Zr(isopropyl)]^+$ can be rationalized by the high stability arising from a *double* β-agostic interaction. It is now straightforward to suggest that a similar effect can occur in the propagation into a *secondary* growing polypropene chain (which can be modeled with a *sec*-butyl group), and this would also explain the decrease in the propagation rate and the occurrence of chain-transfer reactions observed after an occasional regioirregular insertion in poor regiospecific catalysts.

The most likely Zr(isopropyl) to Zr(*n*-propyl) interconversion pathway includes (1) unimolecular β-H transfer to the Zr atom with formation of a Zr−H(2,1-propene) cation, which is stabilized by an agostic interaction between one of the methyl protons and the metal center, and (2) associative displacement with an incoming primary propene molecule.

As a final remark, the existence of a concerted chain conformation rearrangement−monomer coordination channel leading to primary propene insertion into a primary growing chain can contribute to rationalizing the influence of ligand structure on processes of chain transfer and therefore on the molecular weight of the polymer; in fact, the formation of a π-propene, β-agostic chain complex as a precursor of the hydrogen exchange reaction seems to be an unfavored process for highly crowded catalysts. As a consequence, other chain-transfer reactions, possibly with a *unimolecular* course, may occur. Indeed, $H_2C(3\text{-}t\text{-Bu-1-Ind})_2ZrCl_2$, $Me_2C(3\text{-}t\text{-Bu-1-Ind})_2ZrCl_2$, and $(Me_5Cp)_2ZrCl_2$ undergo chain transfer mainly via β-methyl elimination,[6,31] whereas less crowded catalysts as $(Cp)_2ZrCl_2$, *rac*-$[Me_2C(1\text{-Ind})_2]ZrCl_2$, *rac*-$[Me_2C(3\text{-Me-1-Ind})_2]ZrCl_2$, and *rac*-$[Me_2C(3\text{-}Me_3Si\text{-1-Ind})_2]ZrCl_2$ in combination with MAO terminate mainly via β-H elimination.[6,31] Moreover, by increasing the size of the substituent in the position 3 of indene, the molecular weights of polymers produced with *fully regiospecific* catalysts of the type *rac*-$[Me_2C(3\text{-R-1-Ind})_2]ZrCl_2$/MAO (R = Me, Me_3Si-, *t*-Bu) are increased. These experimental data could be rationalized by the lower availability of the monomer to chain transfer in highly hindered catalysts.

Experimental Part

The catalyst precursor *rac*-$Me_2C(3\text{-}tert\text{-butyl-1-indenyl})_2ZrCl_2$ was prepared by Dr. I. Nifant'ev according to the procedure described in ref 6a.

MAO was a commercial 10% solution in toluene (Witco). The zirconocene was prereacted with MAO in toluene for 10 min and pressurized into the polymerization reactor containing propene. The polymerization tests were carried out as follows: 0.4 L of propylene was charged into the 1 L stainless steel autoclave (Büchi) at 30 °C, the temperature of the reactor was brought to 50 °C, and, in quick sequence, the catalyst/cocatalyst mixture was loaded under a nitrogen overpressure, excess pressure was released, and the desired amount of hydrogen (measured into a stainless steel 100 mL vial) was added; the polymerization test was carried out for 1 h at 50 °C and then stopped with CO. The polymers were recovered by evaporating the solvents under vacuum and extracted with refluxing toluene under nitrogen in a Kumagawa extractor to remove catalyst residues, toluene was evaporated, and the polymer was dried at 60 °C under high vacuum.

Proton and carbon spectra were obtained using a Varian 300 spectrometer operating in the Fourier transform mode at 120 °C. The samples were dissolved in $C_2D_2Cl_4$. As reference the residual peak of C_2DHCl_4 in the ^1H spectra (5.95 ppm) and the peak of the *mmmm* pentad in the ^{13}C spectra (21.8 ppm) were used. The carbon spectra were acquired with a 90° pulse and 12 s of delay between pulses. About 3000 transients were stored for each spectrum.

Models and Computational Details. Elements of Chirality. The elements of chirality, which are relevant for the present study, are briefly recalled in order to indicate the used terminology. First of all, upon coordination, the prochiral propene gives rise to nonsuperimposable *si* and *re* coordinations.[32] Another element of chirality is that of the catalytic site, arising from coordinated ligands other than the alkene, the monomer, and the growing chain. For metallocenes with prochiral ligands we used the notation (*R*) or (*S*), in parentheses, according to the Cahn−Ingold−Prelog rules[33,34] extended by Schlögl.[35] Without loss of generality, all the calculations reported here refer to models with the (*R*,*R*) chirality of coordination of the $H_2C(3\text{-}tert\text{-butyl-1-indenyl})_2$ ligand.

Computational Details. Stationary points on the potential energy surface were calculated with the Amsterdam Density Functional (ADF) program system,[36] developed by Baerends et al.[37,38] The electronic configuration of the molecular systems were described by a triple-ζ basis set on zirconium for 4s, 4p, 4d, 5s, and 5p. Double-ζ STO basis sets were used for carbon (2s,2p) and hydrogen (1s), augmented with a single 3d and 2p function, respectively.[39,40] The inner shells on zirconium (including 3d) and carbon (1s) were treated within the frozen core approximation. A set of auxiliary[41] s, p, d, f, and g STO functions, centered on all nuclei, was used in order to fit the molecular density and present Coulomb and exchange potentials accurately in each SCF cycle. Energetics and geometries were evaluated by using the local exchange−correlation potential by Vosko et al.,[42] augmented in a self-consistent manner with Becke's[43] exchange gradient correction and Perdew's[44,45] correlation gradient correction. First-order scalar relativistic corrections were added to total energy.[46,47] A recent

(31) Resconi, L.; Piemontesi, F.; Franciscono, G.; Abis, L.; Fiorani, T. *J. Am. Chem. Soc.* **1992**, *114*, 1025.
(32) Hanson, K. R. *J. Am. Chem. Soc.* **1966**, *88*, 2731.
(33) Cahn, R. S.; Ingold, C.; Prelog, V. *Angew. Chem., Int. Ed. Engl.* **1966**, *5*, 385.
(34) Prelog, V.; Helmchem, G. *Angew. Chem., Int. Ed. Engl.* **1982**, *21*, 567.
(35) Schlögl, K. *Top. Stereochem.* **1966**, *1*, 39.
(36) *ADF 2.3.0*; Vrije Universiteit Amsterdam: Amsterdam, The Netherlands, 1996.
(37) Baerends, E. J.; Ellis, D. E.; Ros, *P. Chem. Phys.* **1973**, *2*, 41.
(38) te Velde, B.; Baerends, E. J. *J. Comput. Phys.* **1992**, *99*, 84.
(39) Snijders, J. G.; Baerends, E. J.; Vernooijs, P. *At. Nucl. Data Tables* **1982**, *26*, 483.
(40) Vernoijs, P.; Snijders, J. G.; Baerends, E. J. *Slater Type Basis Functions for the Whole Periodic System*; Department of Theoretical Chemistry, Free University: Amsterdam, The Netherlands, 1981.
(41) Krijn, J.; Baerends, E. J. *Fit Functions in the HFS Method*; Department of Theoretical Chemistry, Free University: Amsterdam, The Netherlands, 1984.
(42) Vosko, S. H.; Wilk, L.; Nusair, M. *Can. J. Phys.* **1980**, *58*, 1200.
(43) Becke, A. *Phys. Rev. A* **1988**, *38*, 3098.
(44) Perdew, J. P.; Zunger, A. *Phys. Rev. B* **1986**, *33*, 8822.
(45) Perdew, J. P. *Phys. Rev. B* **1986**, *34*, 7406.
(46) Snijders, J. G.; Baerends, E. *J. Mol. Phys.* **1978**, *36*, 1789.

Chart 1

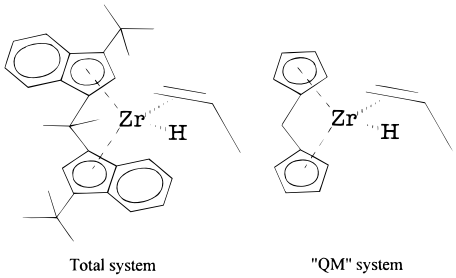

study by Jensen and Børve on Ti ethylene insertion reactions concluded that the functional used in the present paper is well suited to reproduce high-level ab initio coupled cluster calculations for this type of reactions.[48]

The ADF program was modified[49−51] to include standard molecular mechanics force fields in such a way that the QM and MM parts are coupled self-consistently, according to the method prescribed by Morokuma and Maseras.[52] The model QM system and the real QM/MM systems are reported in Chart 1. The partitioning of the systems into QM and MM parts only involves the skeleton of the catalyst's ligand; that is, either the *n*-propyl, the isopropyl, or the monomer is always totally composed by pure QM atoms. Moreover, the metal atom, the hydrogen bonded to it (in models for $[L_2Zr-H(monomer)]^+$), the five-membered Cp rings of the catalysts, and the CH_2 bridge connecting the two Cp rings are also composed by pure QM atoms. The only MM atoms, hence, are the carbon and hydrogen atoms needed to transform the pure QM $H_2C(Cp)_2$ skeleton of the ligand into the CH_2(3-*tert*-butyl-1-indenyl)$_2$ ligand. The connection between the QM and MM parts occurs by means of the so-called capping "dummy" hydrogen atoms, which are present in the model system only.[52] These capping atoms are replaced in the real system by the corresponding "linking" carbon atom.[52]

The QM and MM parts are thus linked by the "capping" hydrogen atoms and coupled by van der Waals interactions. The geometry optimization of the whole system was carried out within this coupling scheme between QM and MM atoms. In the optimization of the MM part, the $C_{cp}-C_{benzene}$ (respectively, $C_{cp}-C_{t-Bu}$) bonds crossing the QM−MM border were kept 0.33 (respectively, 0.41) Å longer than the optimized $C_{cp}-H$ distance. This corresponds to optimized $C-C(sp^2)$ and $C-C(sp^3)$ bond distances roughly equal to 1.43 and 1.51 Å, respectively. Further details on the methodology can be found in previous papers.[49,53]

The molecular mechanics potential was described by the AMBER95 force field;[54] the carbons of the indene system were assigned with atom type "CA", the aromatic ring hydrogen atoms with "HA", and the remaining carbon and hydrogen atoms with "CT" and "HC", respectively. For the atoms that are involved in reactive events at the active site, we followed the convention that atoms whose type changes during a reaction preserve the original type also in the transition state. For example, the propene sp^2 C atoms have a C sp^2 "CA" van der Waals parameter both in the reactant and in the transition state and an sp^3 "CT" one in the products. Electrostatic interactions were not included in the molecular mechanics potential.

All the structures are stationary points on the combined QM/MM potential surface, and no symmetry constraints were used. Geometry optimizations were terminated if the largest component of the Cartesian gradient was smaller than 0.002 au. All reported linear transit calculations involve full geometry optimization along a reaction coordinate that is constrained in each step. Transition state geometries (labeled TS) were approached from the reactant side by a linear-transit procedure, performing full transition state searches starting from geometries corresponding to maxima along the linear-transit curves. At the end of each transition state search, the approximated Hessian presented one negative eigenvalue.

Acknowledgment. We thank S. Tartarini for the polymerization experiments, H. Rychlicki, R. Zeigler, and I. Camurati for the NMR spectra, and L. Cavallo of the University of Naples (Italy) for computational time. Useful discussions on the theoretical subjects of this work with L. Cavallo are gratefully acknowledged.

OM990488G

(47) Snijders, J. G.; Baerends, E. J.; Ros, P. *Mol. Phys.* **1979**, *38*, 1909.
(48) Jensen, V. R.; Børve, K. J. *J. Comput. Chem.* **1998**, *19*, 947.
(49) Deng, L.; Woo, T. K.; Cavallo, L.; Margl, P. M.; Ziegler, T. *J. Am. Chem. Soc.* **1997**, *119*, 6177.
(50) Woo, T. K.; Cavallo, L.; Ziegler, T. *Theor. Chem. Acc.* **1998**, *100*, 307.
(51) Cavallo, L.; Woo, T. K.; Ziegler, T. *Can. J. Chem.* **1998**, *76*, 1457.
(52) Maseras, F.; Morokuma, K. *J. Comput. Chem.* **1995**, *16*, 1170.
(53) Margl, P. M.; Woo, T. K.; Ziegler, T. *Organometallics* **1998**, *17*, 4997.
(54) Cornell, W. D.; Cieplak, P.; Bayly, C. I.; Gould, I. R.; Ferguson, D. M.; Spellmeyer, D. C.; Fox, T.; Caldwell, J. W.; Kollmann, P. A. *J. Am. Chem. Soc.* **1995**, *117*, 5179.